Title	Spin and orbital angular momentum structure of Cu(111) and Au(111) surface states
Auther(s)	Kim, Beomyoung; Kim, Choong H.; Kim, Panjin; Jung, Wonsig; Kim, Yeongkwan; Koh, Yoonyoung; Arita, Masashi; Shimada, Kenya; Namatame, Hirofumi; Taniguchi, Masaki; Yu, Jaejun; Kim, Changyoung
Citation	Physical Review B , 85 (19) : 195402
Issue Date	2012
DOI	10.1103/PhysRevB.85.195402
Self DOI	
URL	http://ir.lib.hiroshima-u.ac.jp/00033907
Right	(c) 2012 American Physical Society
Relation	

Spin and orbital angular momentum structure of Cu(111) and Au(111) surface states

Beomyoung Kim,[1] Choong H. Kim,[2] Panjin Kim,[1] Wonsig Jung,[1] Yeongkwan Kim,[1] Yoonyoung Koh,[1] Masashi Arita,[3] Kenya Shimada,[3] Hirofumi Namatame,[3] Masaki Taniguchi,[3] Jaejun Yu,[2] and Changyoung Kim[1,*]

[1]*Institute of Physics and Applied Physics, Yonsei University, Seoul 120-749, Korea*

[2]*Department of Physics and Astronomy, Seoul National University, Seoul 151-747, Korea*

[3]*Hiroshima Synchrotron Radiation Center, Hiroshima University, Higashi-Hiroshima, Hiroshima 739-0046, Japan*

(Received 12 December 2011; revised manuscript received 2 April 2012; published 2 May 2012)

We performed angle-resolved photoemission studies on Cu(111) and Au(111) surface states with circularly polarized light to investigate local orbital angular momentum (OAM) structures. Existence of OAM is confirmed, as predicted, to exist in systems with an inversion symmetry breaking. Cu(111) surface state bands are found to have chiral OAM in spite of very small spin-orbit coupling, consistent with the theoretical prediction. As for Au(111), we observe split bands for which OAM for the inner and outer bands are parallel, unlike the Bi_2Se_3 case. We also performed first-principles calculations and the results are found to be consistent with experimental results. Moreover, the majority of OAM is found to have d-orbital origin while a small contribution comes from p orbitals. An effective Hamiltonian that incorporates the role of OAM is derived and is used to extract the spin and OAM structures. We discuss the evolution of angular momentum structures from a pure OAM system to a strongly spin-orbit-entangled state. We predict that the transition occurs through a reversal of the OAM direction at a k point in the inner band if the system has a proper spin-orbit coupling strength.

DOI: 10.1103/PhysRevB.85.195402 PACS number(s): 73.20.−r, 79.60.−i, 71.15.Mb

I. INTRODUCTION

When solids possess both inversion and time-reversal symmetries, Kramer's theorem dictates that each electronic state is doubly spin degenerate.[1] When the inversion symmetry is broken at surfaces and interfaces, the spin degeneracy is lifted, except at some special k-space points. The lifting of spin degeneracy and the resulting band splitting in two-dimensional electron gas systems such as metallic surface states are typically explained in terms of the Rahsba effect.[2] In the Rashba model, electron spin interacts with an effective magnetic field stemming from the electron motion in a surface electrostatic field, resulting in a Zeeman splitting. Consequently, the surface-state band splits and attains a chiral spin structure. The band splitting and concomitant chiral spin structure have been experimentally observed in surface states of metals,[3–6] interface states of heterostructures,[7] as well as surface states of topological insulators.[8]

In spite of its success in explaining the energy splitting and chiral spin structure, the original Rashba model could not provide the proper energy scale, giving about 10^5 times smaller value than the measured one in the case of Au(111) surface bands. There have been several theoretical studies to resolve the issue but they did not address all the aspects of the Rashba phenomenon.[9–14] It was only recently found that local orbital angular momentum (OAM) plays the key role in the Rashba-type band splitting by inducing asymmetric charge distribution in Bloch states when the atomic spin-orbit coupling (SOC) is much larger than the crystal-field energy.[15] The asymmetric charge distribution interacts with the surface electrostatic field and provides the energy scale.[10] It results in a chiral OAM structure, and the chiral spin structure naturally follows from the strong SOC. A surprise came when chiral OAM was found to exist even if there is no SOC.[16] In this case, contrary to the strong SOC case, OAM vectors for the degenerate state are found to be parallel to each other while spins are antiparallel.

As discussed above, the spin and OAM configurations, as well as the band splitting, are quite different for the weak and strong SOC cases. It would be interesting to investigate the transition from a weak SOC case to a strong SOC case. To address this issue, we performed angle-resolved photoemission (ARPES) experiments on Cu(111) and Au(111) surface states with circularly polarized light, as well as first-principles calculations. We also develop an effective Hamiltonian to study the problem in an analytical way. We confirm that OAM is indeed present in the Cu(111) and Au(111) surface bands, with most contribution coming from d orbitals. Analysis based on the effective Hamiltonian shows that transition from parallel OAM in the weak SOC case to antiparallel OAM in the strong SOC case occurs through reversal of OAM at a k point in the inner surface band.

II. METHODS

ARPES measurements were performed at the beam line 9A of HiSOR equipped with a VG-SCIENTA R4000 analyzer. Data were taken with right- and left- circularly polarized (RCP and LCP, respectively) 10-eV photons. The total energy resolution was set to be 10 meV at 10 eV, and the angular resolution was 0.1°. We performed experiment at 10 K under a base pressure better than 7.5×10^{-11} Torr. We repeated Ar sputtering and subsequent e-beam heating to obtain clean and well-ordered surfaces. The sample surface was checked by low-energy electron diffraction and its high quality was confirmed through observation of a long-range order. For the density-functional theory (DFT) calculations within the local-density approximation (LDA), we used the OPENMX code[17] based on the linear-combination-of-pseudo-atomic-orbitals (LCPAO) method.[18] Spin-orbit interaction was included via the norm-conserving, fully relativistic j-dependent pseudopotential scheme in the noncollinear DFT formalism.[19] To calculate the spin and OAM for a specific k-point, we used the LCPAO coefficients of

local atoms. Due to the nonorthogonality of pseudoatomic orbitals, LCPAO coefficients are not strictly normalized to unity. To compensate for this, we renormalized the coefficients by assuming the orthogonality and obtained spin and OAM values that are strictly bounded above by 0.5 and 1, respectively.

III. RESULTS AND DISCUSSION

In Fig. 1, we plot ARPES results from Cu(111) surface states. As expected, Cu(111) surface bands are almost degenerate due to the small atomic SOC. The binding energy at the Γ point is $E(\Gamma) = 418$ meV, and the Fermi momentum $k_F = 0.211$ Å^{-1} [see Figs. 1(a)–1(d)]. These values are consistent with the published values.[20] In Fig. 1(e), we plot the circular dichroism (CD) at the Fermi energy defined as CD = RCP − LCP. The CD data presented in the color scale changes gradually from red to blue as value increases continuously from − to +. Plotted in Fig. 1(f) is the cut image along the $k_y = 0$ line shown as the dashed line in Fig. 1(e). This figure shows that CD is negative (positive) for positive (negative) k_y for all energies. The band split near the Γ point is an artifact resulted from broadening in the LCP data due to aging. It is clear from the raw data in Figs. 1(b) and 1(d) that there is only a single band (within the experimental resolution). Finally, plotted in Fig. 1(g) is the normalized CD [defined as NCD = (RCP − LCP)/(RCP + LCP)] at constant binding energies as a function of the azimuthal angle defined in the inset. The curves have a sine function form, which suggests that the OAM forms a chiral structure.[16,21] In addition, the estimated magnitude of OAM from CD decreases as the binding energy increases. The magnitude is found to be approximately proportional to the magnitude of the electron momentum value.

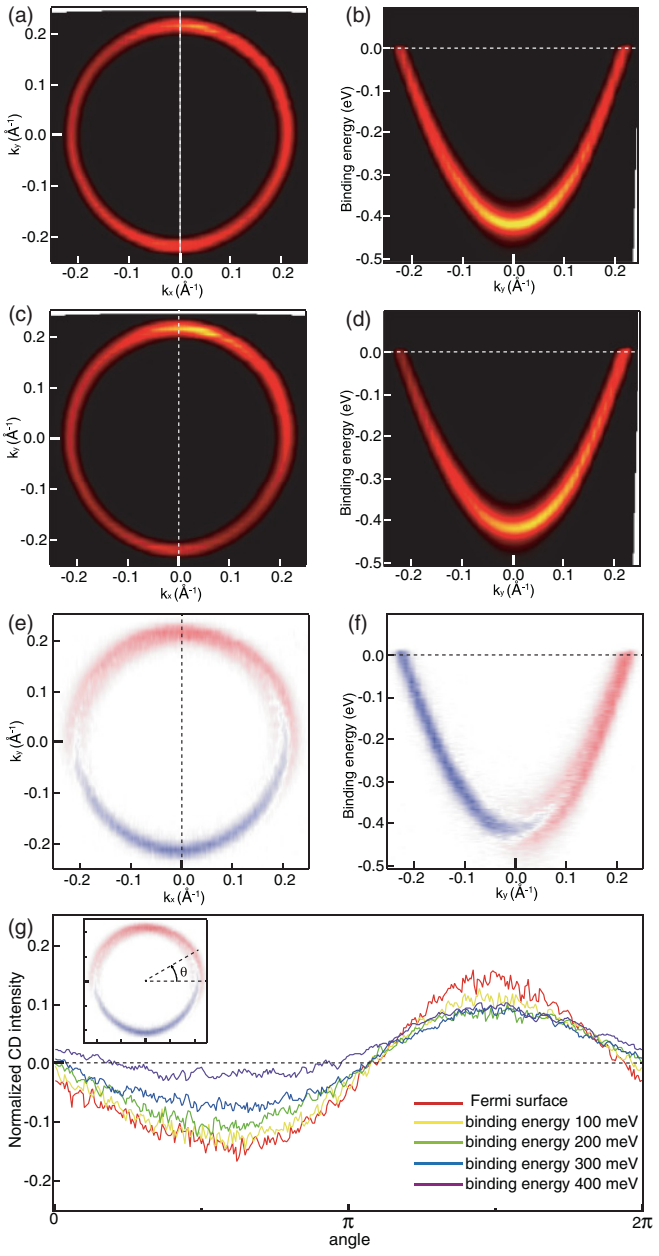

FIG. 1. (Color online) ARPES results from Cu(111) surface states. (a) Fermi surface and (b) the cut along the $k_x = 0$ line [dashed line in panel (a)] taken with RCP light. (c),(d) The same for LCP light. (e),(f) RCP − LCP data. (g) Normalized CD defined as NCD = (RCP − LCP)/(RCP + LCP) as a function of the azimuthal angle defined in the inset.

The behavior of CD in ARPES reveals that chiral OAM indeed exists in the Cu(111) surface band in spite of a very small SOC in Cu.[16] It is also consistent with the prediction that the magnitude of OAM is linear in electron momentum value k. The formation of chiral OAM is a way of lowering the system energy by making the charge distribution asymmetric in the presence of surface electrostatic field.[15] As is discussed later, OAM vectors for the bands are parallel to each other while spins are antiparallel. Note that if CD were due to spins, we would have not observed CD because there is no spin polarization for the states. The fact that we can observe CD from Cu(111) shows that CD comes from the OAM.[16,21,22]

We now turn our attention to the Au(111) surface states, possibly the most studied surface states in regards to the Rashba effect. The first direct experimental evidence for Rashba split bands was from the Au(111) surface.[3] This system has a band shape similar to that of Cu(111) surface states, but has a band splitting of about 110 meV. In Fig. 2(a), we plot Fermi surface map of Au(111) surface states taken with RCP light. Clear double Fermi surfaces due to a Rashba-type splitting are seen in the figure. Figure 2(b) shows the cut along the $k_x = 0$ [dashed line in Fig. 2(a)]. Once again, clear split bands are seen. The observed band bottom is at $E(\Gamma) = 479$ meV and the Fermi vectors are $k_F = 0.165$ Å^{-1} for the inner band and $k_F = 0.196$ Å^{-1} for the outer band. These values are quite consistent with the reported values.[3] Data taken with LCP light in Figs. 2(c) and 2(d) show similar features compared to the RCP data except there is some difference in the intensity profile.

Figures 2(e) and 2(f) plot CD RCP − LCP for the Fermi surfaces and bands along the $k_x = 0$ line [dashed line in 2(e)]. Except that there is clear band splitting, the overall CD profile looks similar to that of Cu(111): It is negative (positive) for the $k_y > 0$ (<0) region. Averaged NCD of the inner and outer bands as a function of the azimuthal angle θ plotted in Fig. 2(g) also shows a similar behavior to that of Cu(111) states. It can be fit with a sine function and the magnitude is approximately

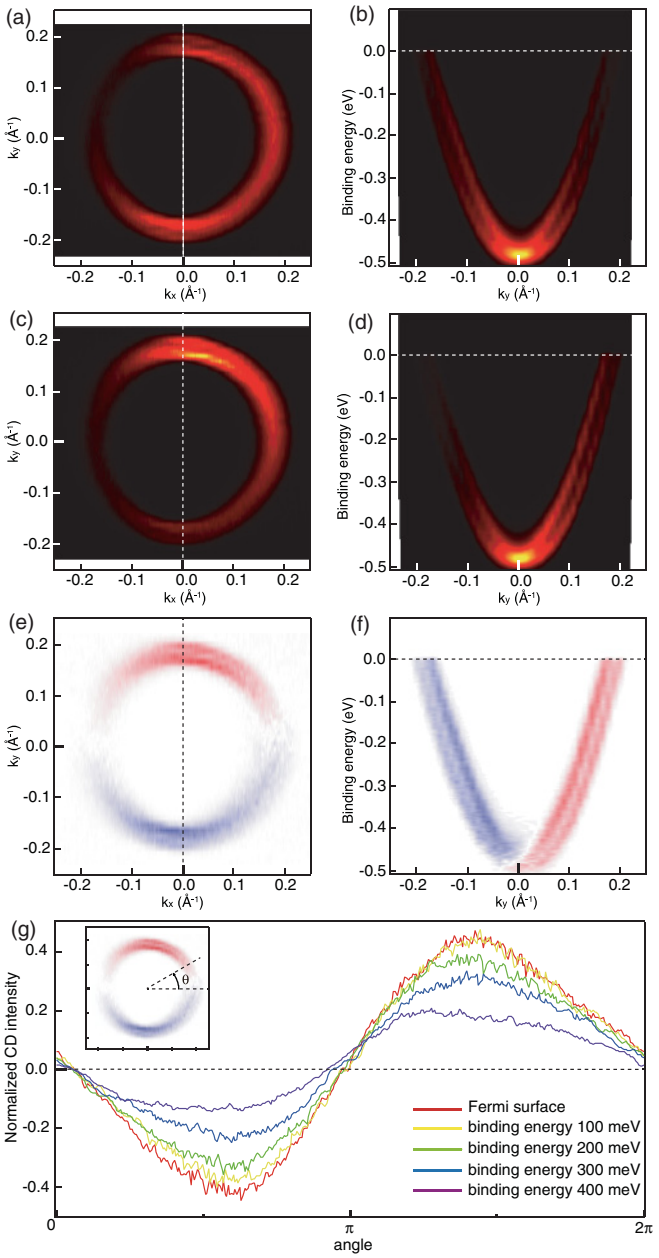

FIG. 2. (Color online) ARPES results from Au(111) surface states. (a) Fermi surface and (b) the cut along the $k_x = 0$ line [dashed line in panel (a)] taken with RCP light. (c),(d) The same for LCP light. (e),(f) RCP − LCP data. (g) NCD as a function of the azimuthal angle. Data from the two bands are summed in the estimation to have averaged NCD.

linear in k. However, we also note that NCD value for Au is about three time larger than that of Cu, which implies that OAM in the Au case is generally larger than that in Cu. A peculiar aspect to note is that, unlike the Bi_2Se_3 case,[21] inner and outer bands have the same CD sign even though their spin directions are supposedly opposite. Same sign of CD suggests that OAM of the inner and outer bands are pointing in the same direction as in the Cu(111) case in spite of a stronger SOC and thus a larger splitting. On the other hand, a careful look reveals that CD for the inner band is slightly stronger (by about 35%) than that from the outer band.

In order to investigate the spin and OAM structures in more detail, we performed first-principles DFT calculations for Au(111) surface states within the LDA. In the DFT results plotted in Fig. 3, top panels [(a) and (b)], show directions and sizes of spin and OAM by the arrows. Panel 3(a) is for the inner band (dashed), while panel 3(b) is for the outer band (solid). The spin and OAM directions obtained from DTF results are as expected. The OAM directions (blue) are parallel to each other for the two bands while spin (red) are opposite to each. The OAM configuration is consistent with the experimental result in Fig. 2.

We turn our attention to the magnitudes of OAM and spin. We first look at the spin magnitude. It is seen from the figures that the spin magnitudes from the two bands are quite similar (only the directions are opposite). Moreover, it has very little momentum dependence. In fact, the magnitude actually slightly decreases as the momentum increases. As for OAM, we find that OAM magnitude increases as we move away from the Γ point, making OAM magnitude approximately linear in k, as indicated in the experimental results. However, the OAM magnitudes for the inner and outer bands are also very similar, which appears to contradict the experimental result.

To better understand the seemingly contradicting results from experiment and theory, we look into atomic orbital dependent contributions to OAM. For Au(111) surface states consist of $5d$ and $6p$ orbitals.[23] In Figs. 3(c) and 3(d), we plot contributions from $5d$ and $6p$ orbitals (green and violet, respectively). One can see that the d-orbital contribution dominates and determines the OAM direction. On the other hand, p-orbital contribution shows quite different behavior from that of d. The direction is opposite for inner and outer bands, making it always antiparallel to the spin direction. Even though the total OAM is similar for the inner and outer bands, they are built differently and result in different CD. As a side note, the composition of the OAM shown in Figs. 3(c) and 3(d) may suggest that the atomic SOC parameter for $6p$ is larger than that of $5d$ because a large value of atomic SOC parameter tends to antialign the spin and OAM.

A natural question is how the spin and OAM structures evolve as a function of SOC strength, from a small SOC (e.g., Cu) to strong SOC (e.g., Bi_2Se_3). To elucidate the issue, we wish to develop an effective Hamiltonian and analyze the evolution. It has already been shown that a free-electron-based model cannot explain various aspects of split bands and that a tight binding state is needed.[9] A through derivation with nearest-neighbor hoppings considered on tight binding states can be found elsewhere.[16] Instead, we wish to develop a simpler effective model for the surface states. For simplicity, we limit our discussion to the p-orbital case, but it can be extended to other orbitals.

For electrons in the surface states, there are four terms that are significant in the Hamiltonian. They are the kinetic energy $\hat{H}_K$, atomic spin orbit coupling $\hat{H}_{\rm SOC}$, crystal field $\hat{H}_{\rm CF}$, and electrostatic energy due to interaction of asymmetric charge distribution with surface electrostatic field $\hat{H}_{\rm ES}$.[15] For the kinetic energy $\hat{H}_K$, we simply add a k^2 term at the end to account for the free-electron-like parabolic band. $\hat{H}_{\rm SOC}$ is $\alpha \vec{L} \cdot \vec{S}$, where α is the atomic SOC parameter. Meanwhile, $\hat{H}_{\rm CF}$ is Δ for p_x and p_z and 0 for p_y (note

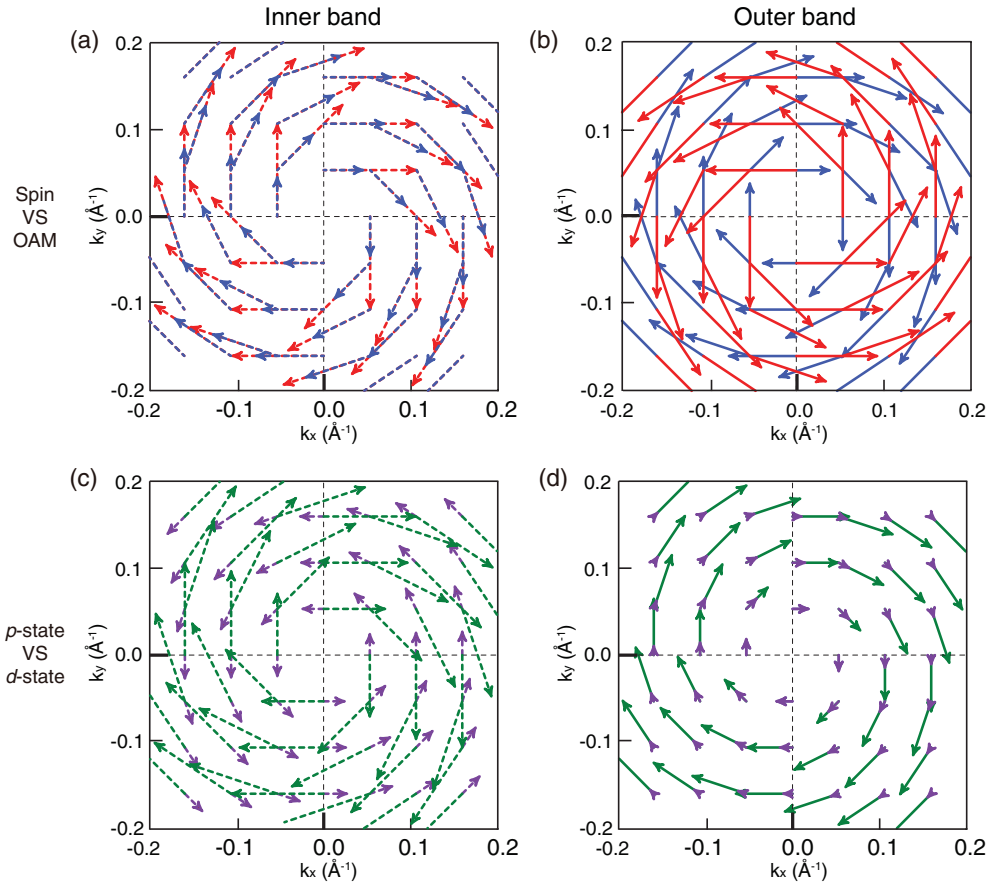

FIG. 3. (Color online) DFT results on the angular momentum structures of Au(111) surface states. DFT results for (a) inner (dashed arrows) and (b) outer bands (solid arrows). OAM (spin) of a state is represented by blue (red) arrows. Shown in the bottom panels are contributions from p state (violet) and d state (green) for (c) inner and (d) outer bands.

that we take y axis as surface normal, not the usual z axis). The last term $\hat{H}_{\rm ES}$ comes from interaction of the surface electrostatic field and electric dipole moment of a state with asymmetric charge distribution.[15] The asymmetric charge distribution is a combined effect of electron momentum and local OAM, and should be proportional to the momentum and OAM. Therefore, the Hamiltonian is given by[15,16] $\hat{H}_{\rm ES} = -\vec{p}\cdot\vec{E}_s = -\alpha_K(\vec{L}\times\vec{k})\cdot\vec{E}_s = -\alpha_K(\vec{k}\times\vec{E}_s)\cdot\vec{L}$, where α_K is a constant that is related to how efficiently asymmetric charge is created by $\vec{k}$ and $\vec{L}$. It is similar to the well-known Rashba Hamiltonian $\hat{H}_R = \alpha_{\rm R}(\vec{k}\times\vec{E}_s)\cdot\vec{\sigma}$ with the spin operator replaced by the OAM operator, but can account for the split energy.

To see how the spin and OAM structures as well as the band splitting evolve as a function of α, we consider a state along the x direction $\vec{k} = k_x\hat{x}$, without loss of generality, in which case $\hat{H}_{\rm ES} = -\alpha_K k_x E_s \hat{L}_z$. The total Hamiltonian is estimated in the basis of $|p_{x\uparrow}\rangle$, $|p_{x\downarrow}\rangle$, $|p_{y\uparrow}\rangle$, $|p_{y\downarrow}\rangle$, $|p_{z\uparrow}\rangle$, and $|p_{z\downarrow}\rangle$. The result is given by

$$\hat{H} = Ck^2\hat{I} + \begin{pmatrix} \Delta & 0 & i\alpha_K k_x E_s - \frac{i\alpha}{2} & 0 & 0 & \frac{\alpha}{2} \\ & \Delta & 0 & i\alpha_K k_x E_s + \frac{i\alpha}{2} & -\frac{\alpha}{2} & 0 \\ & & 0 & 0 & 0 & -\frac{i\alpha}{2} \\ & & & 0 & -\frac{i\alpha}{2} & 0 \\ & & \text{H.c.} & & \Delta & 0 \\ & & & & & \Delta \end{pmatrix}.$$

The 6×6 matrix is diagonalized to obtain the eigenstates and energies. The two lowest energy states correspond to the surface states we have discussed above, and their spin and OAM can be easily estimated.

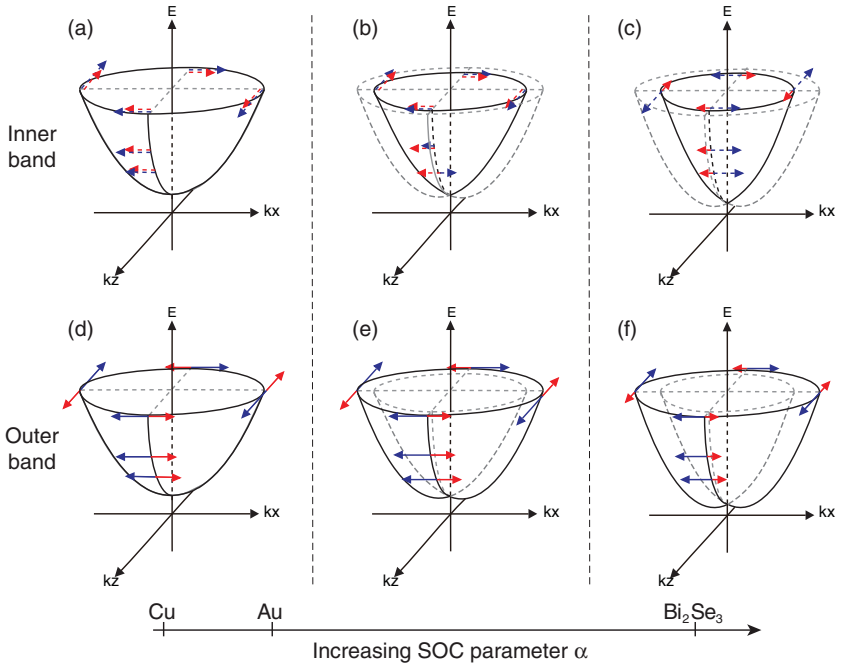

FIG. 4. (Color online) Spin and OAM structures calculated by using the effective Hamiltonian for (a),(d) small, (b),(e) intermediate, and (c),(f) large atomic SOC parameter α. All the parameters are fixed except α. We chose 0.195 $Å^{-1}$ as the Fermi momentum k_F of the outer band, similar to the case of Au(111). The red and blue arrows represent spin and OAM, respectively. Top (bottom) panels are plot spin and OAM configurations for the inner (outer) band. Dashed (solid) arrows are used for the inner (outer) band to be consistent with the notation in Fig. 3. Also marked are the approximate locations of Cu, Au, and Bi_2Se_3 cases on the α asis.

The spin and OAM of the two states are obtained as a function of atomic SOC parameter α to investigate the evolution of spin and OAM. The results are plotted in Fig. 4. Red (blue) color denotes spin (OAM), while dashed (solid) arrows are for the inner (outer) band in the top (bottom) panels. α increases as we go from left to right, and α/α_K values of 0, 0.2, and 3 are used for the three cases. For the $\alpha = 0$ case in Figs. 4(a) and 4(d), the bands are degenerate. The OAM and spin structures are consistent with the results discussed above. The OAM forms a chiral structure with the magnitude approximately linear in k while spins are antiparallel to each other but collinear with the OAM. This case represents the Cu(111) surface states and also somewhat of the Au(111) case (except the band splitting). We also look at the other extreme of a large α case in Figs. 4(c) and 4(f). In this case, the degeneracy is lifted with a large band splitting. The OAM and spin are always antiparallel to each other due to the large α and the magnitude of OAM is independent of the electron momentum k, which is consistent with the results from Bi_2Se_3.[21]

We finally examine the intermediate case in Figs. 4(b) and 4(e), which should provide us information on how parallel OAM for the small α case evolves to antiparallel OAM for the large α case. For the outer band in Fig. 4(e), OAM and spin are antiparallel and the OAM magnitude has a linear k dependence. This is similar to the small α case. The inner band, however, shows a quite different behavior in Fig. 4(b). While OAM and spin are parallel to each other near the Fermi energy, they become antiparallel near the Γ point (small k value). When k increases from 0, OAM gradually decreases, reverses direction and increases again. Therefore, the OAM structure evolves from parallel configuration in the small α case to antiparallel configuration in the large α case by reversing the OAM direction in the inner band at a certain k point instead of reversing the direction at all k points. Such behavior stems from the fact that $\hat{H}_{\mathrm{SOC}}$ is larger than $\hat{H}_{\mathrm{ES}}$ for a small k and OAM prefers to stay antiparallel to the spin. On the other hand, for a large k value, $\hat{H}_{\mathrm{ES}}$ is dominant and the system lowers the energy by inducing parallel OAM as in the Cu(111) case. In the case of Au, such reversal of the OAM in the inner band was not observed, which means α for Au may not be large enough. Observation of such OAM reversal may be possible for surface states of Pb.

IV. SUMMARY

ARPES studies on Cu(111) and Au(111) surface states with circularly polarized light as well as first-principles calculations have been performed to investigate the spin and OAM structures. Experimental and theoretical results show that OAM indeed exists even for Cu(111) and Au(111) surface states, as predicted earlier.[16] Cu(111) has almost degenerate bands with chiral and parallel OAM while Au(111) has split bands with OAM structure not too much different from that of Cu(111). DFT calculation shows that the majority of OAM comes from d states while a small contribution is from p orbitals. We also developed an effective Hamiltonian with the role of OAM incorporated to investigate the evolution of the spin and OAM structures as a function of the atomic SOC parameter. We find that there should be OAM reversal at a specific momentum in the inner band when the system has a proper SOC strength.

ACKNOWLEDGMENTS

This work is supported by NRF (Contract No. 20100018092) and the KICOS under Grant No. K20602000008. J.Y. acknowledges the support through NRF Grant No. R17-2008-033-01000-0 funded by the MEST. This work was performed with the approval of the Proposal Assessing Committee of HSRC (Proposal No.10-A-57).

*changyoung@yonsei.ac.kr

[1]H. A. Kramers, Proc. Acad. Sci. Amsterdam **33**, 959 (1930).
[2]Y. A. Bychkov and E. I. Rashba, JETP Lett. **39**, 78 (1984).
[3]S. LaShell, B. A. McDougall, and E. Jensen, Phys. Rev. Lett. **77**, 3419 (1996).
[4]M. Hoesch, M. Muntwiler, V. N. Petrov, M. Hengsberger, L. Patthey, M. Shi, M. Falub, T. Greber, and J. Osterwalder, Phys. Rev. B **69**, 241401 (2004).
[5]Christian R. Ast and Hartmut Höchst, Phys. Rev. Lett. **87**, 177602 (2001); Yu. M. Koroteev, G. Bihlmayer, J. E. Gayone, E. V. Chulkov, S. Blügel, P. M. Echenique, and Ph. Hofmann, *ibid*. **93**, 046403 (2004); T. Hirahara, K. Miyamoto, I. Matsuda, T. Kadono, A. Kimura, T. Nagao, G. Bihlmayer, E. V. Chulkov, S. Qiao, K. Shimada, H. Namatame, M. Taniguchi, and S. Hasegawa, Phys. Rev. B **76**, 153305 (2007).
[6]D. Pacilé, C. R. Ast, M. Papagno, C. Da Silva, L. Moreschini, M. Falub, Ari P. Seitsonen, and M. Grioni, Phys. Rev. B **73**, 245429 (2006); Christian R. Ast, Jurgen Henk, Arthur Ernst, Luca Moreschini, Mihaela C. Falub, Daniela Pacilé, Patrick Bruno, Klaus Kern, and Marco Grioni, Phys. Rev. Lett. **98**, 186807 (2007); Christian R. Ast, Daniela Pacilé, Luca Moreschini, Mihaela C. Falub, Marco Papagno, Klaus Kern, Marco Grioni, J. Henk, A. Ernst, S. Ostanin, and P. Bruno, Phys. Rev. B **77**, 081407(R) (2008); Fabian Meier, Vladimir Petrov, Sebastian Guerrero, Christopher Mudry, Luc Patthey, Jürg Osterwalder, and J. Hugo Dil, *ibid*. **79**, 241408(R) (2009).
[7]Junsaku Nitta, Tatsushi Akazaki, Hideaki Takayanagi, and Takatomo Enoki, Phys. Rev. Lett. **78**, 1335 (1997)
[8]M. Z. Hasan and C. L. Kane, Rev. Mod. Phys. **82**, 3045 (2010).
[9]L. Petersen and P. Hedegård, Surf. Sci. **459**, 49 (2000).
[10]Miki Nagano, Ayaka Kodama, T. Shishidou, and T. Oguchi, J. Phys.: Condens. Matter **21**, 064239 (2009).
[11]Koichiro Yaji, Yoshiyuki Ohtsubo, Shinichiro Hatta, Hiroshi Okuyama, Koji Miyamoto, Taichi Okuda, Akio Kimura, Hirofumi Namatame, Masaki Taniguchi, and Tetsuya Aruga, Nat. Commun. **1**, 17 (2010).
[12]G. Bihlmayer, S. Blügel, and E. V. Chulkov, Phys. Rev. B **75**, 195414 (2007).
[13]Emmanouil Frantzeskakis, Stéphane Pons, and Marco Grioni, Phys. Rev. B **82**, 085440 (2010).
[14]Tamio Oguchi and Tatsuya Shishidou, J. Phys.: Condens. Matter **21**, 092001 (2009).
[15]Seung Ryong Park, Choong H. Kim, Jaejun Yu, Jung Hoon Han, and Changyoung Kim, Phys. Rev. Lett. **107**, 156803 (2011).
[16]Jin-Hong Park, Choong H. Kim, Jun Won Rhim, and Jung Hoon Han, Phys. Rev. B **85**, 195401 (2012).
[17][http://www.openmx-square.org].
[18]T. Ozaki, Phys. Rev. B **67**, 155108 (2003).
[19]Gerthard Theurich and Nicola A. Hill, Phys. Rev. B **64**, 073106 (2001).
[20]M. Mulazzi, G. Rossi, J. Braun, J. Minár, H. Ebert, G. Panaccione, I. Vobornik, and J. Fujii, Phys. Rev. B **79**, 165421 (2009).
[21]Seung Ryong Park, Jinhee Han, Chul Kim, Yoon Young Koh, Changyoung Kim, Hyungjun Lee, Hyoung Joon Choi, Jung Hoon Han, Kyung Dong Lee, Nam Jung Hur, Masashi Arita, Kenya Shimada, Hirofumi Namatame, and Masaki Taniguchi, Phys. Rev. Lett. **108**, 046805 (2012).
[22]Wonsig Jung, Yeongkwan Kim, Beomyoung Kim, Yoonyoung Koh, Chul Kim, Masaharu Matsunami, Shin-ichi Kimura, Masashi Arita, Kenya Shimada, Jung Hoon Han, Juyoung Kim, Beongki Cho, and Changyoung Kim, Phys. Rev. B **84**, 245435 (2011).
[23]J. Henk, M. Hoesch, J. Osterwalder, A. Ernst, and P. Bruno, J. Phys.: Condens. Matter **16**, 7581 (2004).